Molecular Crystals and Liquid Crystals

Publication details, including instructions for authors and subscription information:
http://www.tandfonline.com/loi/gmcl20

Synthesis and Phase Behavior of New Isoflavone Derivatives: Crystal Structure of 7-Hexyloxy-3-[4′-(3-methylbutyloxy)phenyl]-4H-1-benzopyran-4-one

Guan-Yeow Yeap [a], Wan-Sinn Yam [a], Daisuke Takeuchi [b], Masaki Kakeya [b] & Kohtaro Osakada [b]

[a] Liquid Crystal Research Laboratory, School of Chemical Sciences, Universiti Sains Malaysia, Penang, Malaysia

[b] Chemical Resources Laboratory, Tokyo Institute of Technology, Yokohama, Japan

Version of record first published: 22 Sep 2010

To cite this article: Guan-Yeow Yeap, Wan-Sinn Yam, Daisuke Takeuchi, Masaki Kakeya & Kohtaro Osakada (2008): Synthesis and Phase Behavior of New Isoflavone Derivatives: Crystal Structure of 7-Hexyloxy-3-[4′-(3-methylbutyloxy)phenyl]-4H-1-benzopyran-4-one, Molecular Crystals and Liquid Crystals, 482:1, 87-102

To link to this article: http://dx.doi.org/10.1080/15421400801914723

Mol. Cryst. Liq. Cryst., Vol. 482, pp. 87–102, 2008

ISSN: 1542-1406 print/1563-5287 online
DOI: 10.1080/15421400801914723

Synthesis and Phase Behavior of New Isoflavone Derivatives: Crystal Structure of 7-Hexyloxy-3-[4′-(3-methylbutyloxy)phenyl]-4H-1-benzopyran-4-one

Guan-Yeow Yeap[1], Wan-Sinn Yam[1], Daisuke Takeuchi[2], Masaki Kakeya[2], and Kohtaro Osakada[2]
[1]Liquid Crystal Research Laboratory, School of Chemical Sciences, Universiti Sains Malaysia, Penang, Malaysia
[2]Chemical Resources Laboratory, Tokyo Institute of Technology, Yokohama, Japan

This article describes the synthesis and mesomorophic behavior of a novel homologous series of 7-alkyloxy-3-[4′-(3-methylbutyloxyphenyl)-4H-1-benzopyran-4-one. The title compounds were made up of central isoflavone core with branched and linear alkyloxy terminal chains at C-4′ and C-7, respectively. The influences of linear alkyloxy terminal chain in different length of OR (where $R = C_nH_{2n+1}$; even number of n ranging from 4 to 18) were discussed. The thermal behavior especially the phase transition and respective enthalpy values of the compounds thus synthesized were analyzed using differential scanning calorimetry. The occurrence of mesophases under the polarized light has suggested the molecular orientation and arrangement of the title compounds. The molecular structure of compound 7-hexyloxy-3-[4′-(3methylbutyloxyphenyl)]-4H-1-benzopyran-4-one in crystal phase was confirmed by single-crystal X-ray diffraction of which the space group is P-1(#2) with the lattice parameters $a = 6.100(5)$ Å, $b = 11.704(10)$ Å, $c = 17.082(17)$ Å, $\alpha = 80.85(4)^\circ$, $\beta = 85.56(4)^\circ$, $\gamma = 72.48(3)^\circ$, and $V = 1147.6(18)$ Å^3. The elongated alkyloxy terminal chains were found to be fully stretched in solid phase. All present compounds except the derivative with $R = C_4H_9$ were smectogenic.

Keywords: 7-alkyloxy-3-[4′-(3-methylbutyloxyphenyl)-4H-1-benzopyran-4-one; mesomorphic behavior; single-crystal X-ray diffraction; smectogenic

Received April 25, 2007; accepted July 25, 2007.
Address correspondence to Guan-Yeow Yeap, Liquid Crystal Research Laboratory, School of Chemical Sciences, University Sains Malaysia, Minden, Penang, 11800, Malaysia. E-mail: gyyeap@usm.my or gyyeap_liqcryst_usm@yahoo.com

INTRODUCTION

The mesogenicity of several isoflavone derivatives with classical calamitic structure containing one or two terminal chains have extensively been studied in recent years [1–4]. The introduction of heterocyclic rings within the central core and the linking groups between the middle and the terminal fragments have claimed to be responsible for the liquid crystalline behavior of classical calamitic mesogens leading to various mesomorphism. The relationship between the difference in phase behavior of this type of compounds and their molecular structure has recently been reported in our laboratory of which the anisotropic properties of the molecules were dependent on their polarizability values which in turn corresponded with the occurrence of intermolecular interaction within the mesomorphic region [5]. In this article, we report the synthesis and mesomorphic properties of other newly derived isoflavones 7-alkyloxy-3-[4′-(3-methylbutyloxyphenyl)-4H-1-benzopyran-4-one. A crystal structure of 7-hexyloxy-3-[4′-(3-methyl-butyloxyphenyl)]-4H-1-benzopyran-4-one was confirmed along with Fourier transformed infrared (FTIR) and high resolution nuclear magnetic resonance (^{1}H and ^{13}C NMR) spectroscopy. The phase behavior and texture observation were investigated using differential scanning calorimetry (DSC) and polarizing optical microscope (POM). The synthetic routes towards the formation of the intermediates and title compounds were shown in Scheme 1.

EXPERIMENTAL

4-Hydroxyphenylacetic acid, 1-bromo-3-methylbutane (Acros), resorcinol (Aldrich), methanesulfonyl chloride, boron trifluoride, potassium carbonate, 1-bromobutane, 1-bromohexane, 1-bromooctane, 1-bromodecane, 1-bromododecane, 1-bromotetradecane, 1-bromohexadecane and 1-bromooctadecane (Merck) were used directly without further purification.

Thin-layer chromatography analyses were performed using aluminium-backed silica-gel plates (Merck 60 F254) and were examined under UV light. Column chromatography was performed under gravity using Merck 60-mesh silica gel.

Microanalyses for all the final compounds **4–11** were carried out on 2400 LS Series CHNS/O analyzer.

The FTIR data were recorded using a Perkin Elmer 2000-FTIR spectrophotometer in the frequency range 4000-400 cm^{-1} with samples prepared in KBr pellets. The bands associated with the stretching vibrations of aliphatic C-H, C=O pyranone and C=C in compounds

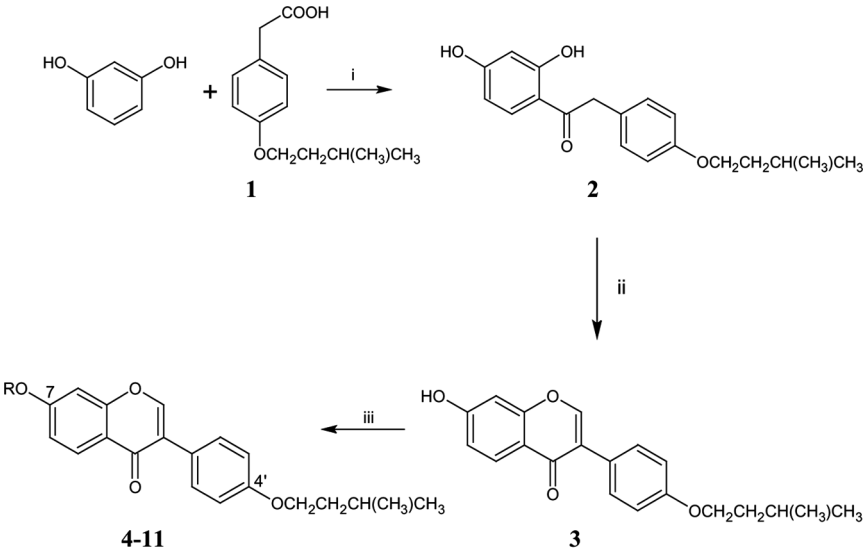

Compound	R
4	C_4H_9
5	C_6H_{13}
6	C_8H_{17}
7	$C_{10}H_{21}$
8	$C_{12}H_{25}$
9	$C_{14}H_{29}$
10	$C_{16}H_{33}$
11	$C_{18}H_{37}$

SCHEME 1 Synthetic route towards the formation of intermediates (**2**, **3**) and title compounds **4–11**. Reagents and conditions: (i) BF_3/Et_2O heat at 70–75°C for 4h; (ii) N_2 atmosphere, DMF, BF_3/Et_2O heat at 55°C for 1 h; $MeSO_2Cl$ heat for 1.5 h; (iii) RBr (R=C_nH_{2n+1} and n are even numbers ranging from 4 to 18); K_2CO_3/acetone; reflux overnight.

4–11 were observed in their respective FTIR spectra ($\nu_{C-H} =$ 2850–2957 cm^{-1}, $\nu_{C=O} =$ 1631–1633 cm^{-1}, and $\nu_{C=C} =$ 1256–1258 cm^{-1}).

NMR (^1H and ^{13}C) analyses were performed by a Bruker 400 MHz ultrashield spectrometer. Deuterated chloroform ($CDCl_3$) and dimethylsulphoxide (DMSO-d_6) were used as solvents and TMS as internal standard. The NMR spectra for all members of the homologous series exhibit similar trend in ^1H-^1H splitting and chemical shifts. Aromatic protons are observed within the chemical shift (δ) range of 6.82–8.23 ppm whereas the triplets observed at $\delta =$ 4.04–4.06 ppm and 4.00–4.03 ppm for the compounds **4–11** can be

ascribed to the OCH_2 attached to C-7 and C-4′ at the respective ether linkages. The signals due to the methylene and methine protons in the branched alkyloxy chain at C-4′ were overlapped within $\delta = 1.80$–1.91 ppm. The resonances in relation to two methyl protons in the branched alkyloxy chain appear as doublet within $\delta = 0.97$–0.99. Multiplets and triplets within the $\delta = 1.26$–1.80 ppm and 0.88–0.96 ppm can be attributed to the presence of methylene and methyl protons of the linear alkyloxy terminal chain attached to C-7. Inspection from the ^{13}C NMR spectra shows the peaks at $\delta = 175.89$–176.29 ppm owing to the presence of pyranone C=O. The presence of peaks at 66.45–69.15 ppm indicates the presence of ether groups.

The phase transition temperatures and enthalpy values were measured by Seiko DSC6200R differential scanning calorimetry at heating and cooling rate of $5^{\circ}C\ min^{-1}$ and $-5^{\circ}C\ min^{-1}$, respectively. The textures of the mesophases were studied using a Carl Zeiss polarizing microscope attached with a Linkam LTS350 hot stage and temperature controller. The samples studied by optical microscopy were prepared in thin film sandwiched between glass slide and cover. The thermal behavior was studied via the enthalpy values expressed in $kJ\ mol^{-1}$.

The molecular simulation using the ACD/Chemsketch Version 4.5 has been carried out in order to acquire the information with respect to the molecular conformation and geometry. The refinement on the conformation can be achieved through the geometrical optimization or energy minimization upon the molecule prior to obtain the polarizability of each compound.

X-Ray Crystal Structure Analysis for Compound 5

A colorless prism crystal of $C_{26}H_{32}O$ having approximate dimensions of $0.17 \times 0.15 \times 0.10$ m was mounted on a glass fiber. All measurement were carried out on a Crystal Clear (Rigaku) Saturn CCD area detector with graphite monochromated Mo-Kα radiation, ($\lambda = 0.71070$ Å) with the aid of CrystalStructure and related software [6,7] to a maximum 2θ value of 54.8°. Cell constants and an orientation matrix for data collection corresponded to a primitive triclinic cell. Data were collected at a temperature of $-160 \pm 1^{\circ}C$. A total of 720 oscillation images were collected. A sweep of data was done using ω scans from -110.0 to 70.0° in 0.5° step, at $\chi = 45.0^{\circ}$ and $\phi = 0.0^{\circ}$. The exposure rate was 100.0 [sec/°]. The detector swing angle was -20.07°. A second sweep was performed using ω scans from -110.0 to 70.0° in 0.5° step, at $\chi = 45.0^{\circ}$ and 90.0° with the same exposure rate and detector swing angle. Readout was performed in the 0.547 mm pixel mode.

Of the 6347 reflections that were collected, 3982 were unique ($R_{int} = 0.036$); equivalent reflections were merged. Data were collected and processed using Crystal Clear (Rigaku). The linear absorption coefficient, μ, for Mo-Kα radiation is $0.781\,cm^{-1}$. An empirical absorption correction was applied which resulted in transmission factors from 0.739 to 0.992. The data were collected for Lorentz and polarization effects. The structure was solved by direct methods [8] and expanded using Fourier techniques [9]. The nonhydrogen atoms were refined anisotropically. Hydrogen atoms were refined using the riding model. The final cycle of full-matrix least-squares refinement on F^2 was based on 1916 observed reflections and 303 variable parameters and converged (largest parameter shifts was 0 times its esd) with unweighted and weighted agreement factors of $R_1 = 0.0823$ and $wR_2 = 0.2121$. The standard deviation of an observation of unit weight was 1.00. A Sheldrick weighting scheme was used. Plots of $\Sigma w(|F_o| - |F_c|)^2$ *versus* $|F_o|$, reflection order in data collection, sin θ/λ, and various classes of indices showed no unusual trends. The maximum and minimum peaks on the final difference Fourier map corresponded to 0.51 and $-0.31\,e\text{Å}^{-3}$, respectively.

Neutral atom scattering factors were taken from Cromer and Waber [10]. Anomalous dispersion effects were included in Fcalc [11]; the values for $\Delta f'$ and $\Delta f''$ were those of Creagh and McAuley [12]. The values for the mass attenuation coefficients are those of Creagh and Hubbell [13].

Synthesis

The synthesis of the intermediates **1–3** and the ultimate compounds **4–11** were carried out using the experimental procedure described in Scheme 1.

Synthesis of 4-(3-Methylbutyloxy)phenylacetic Acid, 1

To a cold solution containing 10.0 g of 4-hydroxybenzoic acid in 25.0 ml of methanol, 7.4 g of potassium hydroxide in 25.0 ml of methanol was added. The ice bath was then removed and 10.1 g of 1-bromo-3-methylbutane was added and the reaction mixture was heated under reflux for 18 h. The solvent was subsequently removed and the mixture was neutralized with 10% of aqueous hydrochloric acid. The solid was filtered off, washed thoroughly with water and recrystallized from methanol. Yield: 75%. IR (KBr)/cm^{-1} 2957, 2933, 2868 (CH_2 aliphatic), 1695 (C=O), 1616 (C=C aromatic), and 1246 (C-O).

Synthesis of 1-(2,4-Dihydroxyphenyl)-2-[4′-(3-methylbutyloxyphenyl)]-ethanone, 2

A mixture containing 9.0 g of 4-(3-methylbutyloxy)phenylacetic acid and 4.5 g of resorsinol in 82.0 ml $BF_3 \cdot Et_2O$ was heated for 4 h at 70–75°C under nitrogen atmosphere. The resulting mixture was later poured into an ice-water bath whereupon the precipitate formed. The oil was separated, air dried, and purified using chloroform. Yield: 70%. IR (KBr)/cm^{-1} 3126 (OH), 2957, 2873 (CH_2 aliphatic), 1625 (C=O), 1611 (C=C aromatic), and 1249 (C-O).

Synthesis of 7-Hydroxy-3-[4′-(3-methylbutyloxyphenyl)]-4H-1-benzopyran-4-one, 3

Seven grams of compound **2** in dry DMF was treated cautiously with 4-equivalence of $BF_3 \cdot Et_2O$. To this mixture, 3-equivalence of $MeSO_2Cl$ was added at 50°C. The mixture was further heated under nitrogen atmosphere for 1.5 h at 75–80°C. Subsequently, the mixture was poured with rapid stirring into ice-water bath whereupon the solid formed. The product was purified via recrystallization from chloroform. Yield: 45%. IR (KBr)/cm^{-1} 3206 (OH), 1628 (C=O), 1610 (C=C aromatic) and 1246 (C-O). ^{1}H-NMR (DMSO-d_6) δ/ppm 12.79 (s, 7-OH), 9.58 (s, 4′-OH), 6.72–8.27 (8H, Ar-H), 4.04–4.06 (2H, d, OCH_2), 1.83–1.89 (3H, m, $OCH_2C\underline{H}_2C\underline{H}(CH_3)CH_3$), 0.99 (6H, d, $OCH_2CH_2CH(C\underline{H}_3)C\underline{H}_3$). ^{13}C-NMR (DMSO-$d_6$) δ/ppm 176.32 (C=O), 163.93 (OH attached to C-7), 159.52–100.89 (C aromatic), aliphatic chains: 66.59 (C-O), 37.83 ($OCH_2CH_2\underline{C}H(CH_3)CH_3$), 31.70 ($\underline{C}H_2CH_2O$) and 22.69 ($OCH_2CH_2CH(\underline{C}H_3)\underline{C}H_3$)

Synthesis of 7-Alkyloxy-3-[4′-(3-methylbutyloxyphenyl)]-4H-1-benzopyran-4-one, 4–11

To a mixture containing 0.3 g of compound **3** in acetone, 2.5 equivalence of potassium carbonate and 1.2 equivalence of the corresponding 1-bromoalkane were added. The mixture was heated under reflux for 12 h. The solvent was removed and the crude product was purified using column chromatography with chloroform:ethyl acetate (9:1) as eluent. The analytical data for compounds 4–11 are shown as follows.

Compound **4**: Yield: 33%. Elemental analysis found: C, 82.94; H, 8.57%. Calculated: C, 82.90; H, 8.58%. IR (KBr)/cm^{-1} 2957, 2923, 2856 (CH_2 aliphatic), 1633 (C=O), 1606 (C=C aromatic), 1257 (CO). ^{1}H-NMR ($CDCl_3$) δ/ppm 6.83–8.21 (8H, H-Ar), 4.04–4.06 (2H, t, OCH_2 attached to C-7), 4.01–4.03 (2H, t, OCH_2 attached to C-4′), 1.84–1.91 (3H, m, $OCH_2C\underline{H}_2C\underline{H}(CH_3)CH_3$), 1.69–1.76 (2H, m, $C\underline{H}_2$-CH_2O), 1.40–1.58 (2H, m, $OCH_2CH_2C\underline{H}_2CH_3$), 0.98 (6H, d,

$OCH_2CH_2CH(C\underline{H}_3)C\underline{H}_3$), 0.94–0.96 (3H, t, $OCH_2CH_2(CH_2)_7C\underline{H}_3$). ^{13}C-NMR ($CDCl_3$) δ/ppm 176.24 (C=O), 163.58–100.76 (C aromatic), 69.15 (OCH_2 attached to C-7), 66.96 (OCH_2 attached to C-4′), 37.89 ($OCH_2CH_2\underline{C}H(CH_3)CH_3$), 23.68–32.06 ($OCH_2\underline{C}H_2\underline{C}H_2CH_3$, $OCH_2\underline{C}H_2CH(CH_3)CH_3$), 22.62 ($OCH_2CH_2CH(\underline{C}H_3)\underline{C}H_3$), 14.10 ($CH_3$).

Compound **5**: Yield: 36%. Elemental analysis found: C, 83.12; H, 8.97%. Calculated: C, 83.32; H, 8.98%. IR (KBr)/cm^{-1} 2954, 2922, 2854 (CH_2 aliphatic), 1632 (C=O), 1607 (C=C aromatic), 1257 (CO). ^{1}H-NMR ($CDCl_3$) δ/ppm 6.85–8.23 (8H, H-Ar), 4.06–4.09 (2H, t, OCH_2 attached to C-7)), 4.03–4.06 (2H, t, OCH_2 attached to C-4′), 1.82–1.90 (3H, m, $OCH_2C\underline{H}_2C\underline{H}(CH_3)CH_3$), 1.69–1.74 (2H, m, $C\underline{H}_2$-CH_2O), 1.36–1.56 (6H, m, $OCH_2CH_2(C\underline{H}_2)_3CH_3$), 0.99 (6H, d, $OCH_2CH_2CH(C\underline{H}_3)C\underline{H}_3$), 0.93–0.96 (3H, t, $OCH_2CH_2(CH_2)_7C\underline{H}_3$). ^{13}C-NMR ($CDCl_3$) δ/ppm 176.25 (C=O), 163.93-100.68 (C aromatic), 69.13 (OCH_2 attached to C-7), 66.82 (OCH_2 attached to C-4′), 38.08 ($OCH_2CH_2\underline{C}H(CH_3)CH_3$), 23.28–32.30 ($OCH_2\underline{C}H_2(\underline{C}H_2)_3CH_3$, $OCH_2\underline{C}H_2CH(CH_3)CH_3$), 22.68 ($OCH_2CH_2CH(\underline{C}H_3)\underline{C}H_3$), 14.51 ($CH_3$).

Compound **6**: Yield: 42%. Elemental analysis found: C, 83.28; H, 9.32%. Calculated: C, 83.11; H, 9.30%. IR (KBr)/cm^{-1} 2956, 2923, 2854 (CH_2 aliphatic), 1632 (C=O), 1607 (C=C aromatic), 1256 (CO). ^{1}H-NMR ($CDCl_3$) δ/ppm 6.83–8.21 (8H, H-Ar), 4.04–4.06 (2H, t, OCH_2 attached to C-7), 4.01–4.03 (2H, t, OCH_2 attached to C-4′), 1.80–1.89 (3H, m, $OCH_2C\underline{H}_2C\underline{H}(CH_3)CH_3$), 1.67–1.72 (2H, m, $C\underline{H}_2-CH_2O$), 1.30–1.50 (10H, m, $OCH_2CH_2(C\underline{H}_2)_5CH_3$), 0.97 (6H, d, $OCH_2CH_2CH(C\underline{H}_3)C\underline{H}_3$), 0.88–0.91 (3H, t, $OCH_2CH_2(CH_2)_5C\underline{H}_3$). ^{13}C-NMR ($CDCl_3$) δ/ppm 175.94 (C=O), 163.55-100.56 (C aromatic), 68.73 (OCH_2 attached to C-7), 66.45 (OCH_2 attached to C-4′), 37.99 ($OCH_2CH_2\underline{C}H(CH_3)CH_3$), 22.66–31.80 ($OCH_2\underline{C}H_2(\underline{C}H_2)_5CH_3$, $OCH_2\underline{C}H_2CH(CH_3)CH_3$), 22.60 ($OCH_2CH_2CH(\underline{C}H_3)\underline{C}H_3$), 14.10 ($CH_3$).

Compound **7**: Yield: 45%. Elemental analysis found: C, 83.43; H, 9.63%. Calculated: C, 83.32; H, 9.61%. IR (KBr)/cm^{-1} 2957, 2922, 2852 (CH_2 aliphatic), 1631 (C=O), 1607 (C=C aromatic), 1257 (CO). ^{1}H-NMR ($CDCl_3$) δ/ppm 6.83–8.21 (8H, H-Ar), 4.04–4.06 (2H, t, OCH_2 attached to C-7), 4.01–4.03 (2H, t, OCH_2 attached to C-4′), 1.80–1.87 (3H, m, $OCH_2C\underline{H}_2C\underline{H}(CH_3)CH_3$), 1.67–1.72 (2H, m, $C\underline{H}_2$-CH_2O), 1.28–1.50 (14H, m, $OCH_2CH_2(C\underline{H}_2)_7CH_3$), 0.97 (6H, d $OCH_2CH_2CH(C\underline{H}_3)C\underline{H}_3$), 0.87–0.90 (3H, t, $OCH_2CH_2(CH_2)_7C\underline{H}_3$). ^{13}C-NMR ($CDCl_3$) δ/ppm 176.29 (C=O), 163.93-100.95 (C aromatic), 69.16 (OCH_2 attached to C-7), 66.83 (OCH_2 attached to C-4′), 38.38 ($OCH_2CH_2\underline{C}H(CH_3)CH_3$), 23.08–32.29 ($OCH_2\underline{C}H_2(\underline{C}H_2)_7CH_3$, $OCH_2\underline{C}H_2CH(CH_3)CH_3$), 22.99 ($OCH_2CH_2CH(\underline{C}H_3)\underline{C}H_3$), 14.51 ($CH_3$).

Compound **8**: Yield: 40%. Elemental analysis found: C, 83.55; H, 9.90%. Calculated: C, 83.58; H, 9.89%. IR (KBr)/cm^{-1} 2957, 2922,

2851 (CH_2 aliphatic), 1631 (C=O), 1607 (C=C aromatic), 1256 (CO). ^{1}H-NMR ($CDCl_3$) δ/ppm 6.83–8.21 (8H, H-Ar), 4.04–4.06 (2H, t, OCH_2 attached to C-7), 4.01–4.03 (2H, t, OCH_2 attached to C-4′), 1.82–1.85 (3H, m, $OCH_2C\underline{H}_2C\underline{H}(CH_3)CH_3$), 1.68–1.72 (2H, m, $C\underline{H}_2$-CH_2O), 1.27–1.48 (18H, m, $OCH_2CH_2(C\underline{H}_2)_9CH_3$), 0.97 (6H, d, $OCH_2CH_2CH(C\underline{H}_3)C\underline{H}_3$), 0.86–0.90 (3H, t, $OCH_2CH_2(CH_2)_9C\underline{H}_3$). ^{13}C-NMR ($CDCl_3$) δ/ppm 175.89 (C=O), 163.57-100.63 (C aromatic), 68.76 (OCH_2 attached to C-7), 66.50 (OCH_2 attached to C-4′), 38.03 ($OCH_2CH_2\underline{C}H(CH_3)CH_3$), 22.70–31.93 ($OCH_2\underline{C}H_2(\underline{C}H_2)_9CH_3$, $OCH_2\underline{C}H_2CH(CH_3)CH_3$), 22.60 ($OCH_2CH_2CH(\underline{C}H_3)\underline{C}H_3$), 14.11 ($CH_3$).

Compound **9**: Yield: 48%. Elemental analysis found: C, 83.67; H, 10.14%. Calculated: C, 83.63; H, 10.13%. IR (KBr)/cm^{-1} 2956, 2920, 2850, (CH_2 aliphatic), 1631 (C=O), 1607 (C=C aromatic), 1258 (CO). ^{1}H-NMR ($CDCl_3$) δ/ppm 6.83–8.21 (8H, H-Ar), 4.04–4.06 (2H, t, OCH_2 attached to C-7), 4.01–4.03 (2H, t, OCH_2 attached to C-4′), 1.82–1.87 (3H, m, $OCH_2C\underline{H}_2C\underline{H}(CH_3)CH_3$), 1.67–1.80 (2H, m, $C\underline{H}_2-CH_2O$), 1.26–1.50 (22H, m, $OCH_2CH_2(C\underline{H}_2)_{11}CH_3$), 0.97 (6H, d, $OCH_2CH_2CH(C\underline{H}_3)C\underline{H}_3$), 0.86–0.90 (3H, t, $OCH_2CH_2(CH_2)_{11}C\underline{H}_3$). ^{13}C-NMR ($CDCl_3$) δ/ppm 176.27 (C=O), 163.92-100.94 (C aromatic), 69.11 (OCH_2 attached to C-7), 66.82 (OCH_2 attached to C-4′), 38.37 ($OCH_2CH_2\underline{C}H(CH_3)CH_3$), 23.08–32.31 ($OCH_2\underline{C}H_2(\underline{C}H_2)_{11}CH_3$, $OCH_2\underline{C}H_2CH(CH_3)CH_3$), 22.98 ($OCH_2CH_2CH(\underline{C}H_3)\underline{C}H_3$), 14.50 ($CH_3$).

Compound **10**: Yield: 42%. Elemental analysis found: C, 83.77; H, 10.36%. Calculated: C, 83.73; H, 10.38%. IR (KBr)/cm^{-1} 2957, 2921, 2850 (CH_2 aliphatic), 1631 (C=O), 1607 (C=C aromatic), 1256 (CO). ^{1}H-NMR ($CDCl_3$) δ/ppm 6.83–8.21 (8H, H-Ar), 4.04–4.06 (2H, t, OCH_2 attached to C-7), 4.00–4.03 (2H, t, OCH_2 attached to C-4′), 1.82–1.89 (3H, m, $OCH_2C\underline{H}_2C\underline{H}(CH_3)CH_3$), 1.69–1.72 (2H, m, $C\underline{H}_2-CH_2O$), 1.26–1.52 (26H, m, $OCH_2CH_2(C\underline{H}_2)_{13}CH_3$), 0.97 (6H, d, $OCH_2CH_2CH(C\underline{H}_3)C\underline{H}_3$), 0.82–0.88 (3H, t, $OCH_2CH_2(CH_2)_{13}C\underline{H}_3$). ^{13}C-NMR ($CDCl_3$) δ/ppm 175.89 (C=O), 163.54-100.56 (C aromatic), 68.73 (OCH_2 attached to C-7), 66.45 (OCH_2 attached to C-4′), 37.99 ($OCH_2CH_2\underline{C}H(CH_3)CH_3$), 22.70–31.94 ($OCH_2\underline{C}H_2(\underline{C}H_2)_{13}CH_3$, $OCH_2\underline{C}H_2CH(CH_3)CH_3$), 22.60 ($OCH_2CH_2CH(\underline{C}H_3)\underline{C}H_3$), 14.13 ($CH_3$).

Compound **11**: Yield: 43%. Elemental analysis found: C, 83.86; H, 10.56%. Calculated: C, 83.84; H, 10.54%. IR (KBr)/cm^{-1} 2954, 2922, 2854, (CH_2 aliphatic), 1631 (C=O), 1607 (C=C aromatic), 1257 (CO). ^{1}H-NMR ($CDCl_3$) δ/ppm 6.82–8.21 (8H, H-Ar), 4.04–4.06 (2H, t, OCH_2 attached to C-7), 4.00–4.03 (2H, t, OCH_2 attached to C-4′), 1.82–1.88 (3H, m, $OCH_2C\underline{H}_2C\underline{H}(CH_3)CH_3$), 1.67–1.80 (2H, m, $C\underline{H}_2$-CH_2O), 1.26–1.51 (30H, m, $OCH_2CH_2(CH_2)_{15}CH_3$), 0.97 (6H, d, $OCH_2CH_2CH(C\underline{H}_3)C\underline{H}_3$), 0.86–0.90 (3H, t, $OCH_2CH_2(CH_2)_{15}C\underline{H}_3$). ^{13}C-NMR ($CDCl_3$) δ ppm 175.89 (C=O), 163.54-100.56 (C aromatic),

68.73 (OCH_2 attached to C-7), 66.45 (OCH_2 attached to C-4′), 37.99 ($OCH_2CH_2\underline{C}H(CH_3)CH_3$), 22.70–31.94 ($OCH_2\underline{C}H_2(\underline{C}H_2)_{15}CH_3$, $OCH_2\underline{C}H_2CH(CH_3)CH_3$), 22.60 ($OCH_2CH_2CH(\underline{C}H_3)\underline{C}H_3$), 14.12 ($CH_3$).

RESULTS AND DISCUSSION

Thermal Behavior and Texture Observation for Compounds 4–11

The phase transition temperatures and their respective enthalpy values obtained from DSC measurement are collated in Table 1. The DSC thermogram for compound **4** exhibits only one transition temperature during heating and cooling processes. This observation indicates the absence of liquid crystalline properties in compound **4** in similar manner to a main chain polymer containing banana-shaped mesogens and dodecyl spacers [14]. The clearing temperature for compound **4** is also found to be highest among the members within this series. This phenomenon can be ascribed to the presence of intermolecular attraction force among short-chain molecules leading to a restricted thermal motion [14,15].

Whilst compounds **5** and **6** are monotropic, the compounds **7–11** exhibit enantiotropic behaviors. Through heating process we can

TABLE 1 Transition Temperatures and Enthalpies for 7-Alkyloxy-3-[4′-(3-Methyl-Butyloxyphenyl)]-4H-1-Benzopyran-4-ones

Compound	Transition temperatures/°C (Enthalpy changes/kJmol^{-1}) – Heating Cooling
4	Cr 148.0 (25.00) I
	I 130.4 (23.29) Cr
5	Cr 152.2 (39.20) I
	I 139.6 (5.49) SmA 135.5 (34.75) Cr
6	Cr 147.1 (21.41) I
	I 142.0(7.21) SmA 132.0 (35.39) Cr
7	Cr 133.6 (33.25) SmA 141.0 (7.84) I
	I 139.2 (8.17) SmA 107.4 (33.98) Cr
8	Cr 136.2 (40.42) SmA 139.4 (8.04) I
	I 137.9 (9.09) SmA 117.3 (43.49) Cr
9	Cr 129.1 (38.0) SmA 136.6 (7.96) I
	I 134.8 (8.13) SmA 99.4 (38.36) Cr
10	Cr 125.9 (42.35) SmA 133.5 (8.47) I
	I 131.7 (8.56) SmA 94.1 (44.35) Cr
11	Cr 123.7 (40.92) SmA 129.2 (7.88) I
	I 127.7 (7.90) SmA 93.8 (45.84) Cr

observe a gradual decrease in clearing temperature (T_c) when we ascend from compounds **7** to **11** (Table 1). This observation agrees with the previously reported homologous series N,N'-bis(3-methoxy-4-alkyloxybenzylidene)-1,4-phenylenediamin in which the homolog with the longest terminal chains was nonlinear leading to lower clearing temperature [16]. The phenomenon can also be explained in terms of dilution effect of the flexible chains as reported for a series of laterally branched azobenzenes [17]. This phenomenon indicates that the dependence of the molecular anisotropy upon the molecular length and hence the polarizability as reported for Schiff base esters [18] is not applicable for the present compounds **5–11**. This has been well reflected by the polarizability values of the compounds **5–11** in which the values for **5** $[(50.01 \pm 0.5) \times 10^{-24}\,\mathrm{cm}^{-3}] <$ **6** $[(53.69 \pm 0.5) \times 10^{-24}\,\mathrm{cm}^{-3}] <$ **7** $[(57.36 \pm 0.5) \times 10^{-24}\,\mathrm{cm}^{-3}] <$ **8** $[(61.03 \pm 0.5) \times 10^{-24}\,\mathrm{cm}^{-3}] <$ **9** $[(64.70 \pm 0.5) \times 10^{-24}\,\mathrm{cm}^{-3}] <$ **10** $[(68.37 \pm 0.5) \times 10^{-24}\,\mathrm{cm}^{-3}] <$ **11** $[(72.04 \pm 0.5) \times 10^{-24}\,\mathrm{cm}^{-3}]$ in spite of the clearing temperatures change in the reverse order (T_c for **5** > **6** > **7** > **8** > **9** > **10** > **11**).

The clearing temperatures for all the compounds **5–11** in this homologous series are generally high (>110.0°C) and this observation can be due to the increased polarity of the endocyclic O atom in the central core which enhances the anisotropy properties. However, the thermal mesomorphic range was small (<10°C) which can be rationalized in

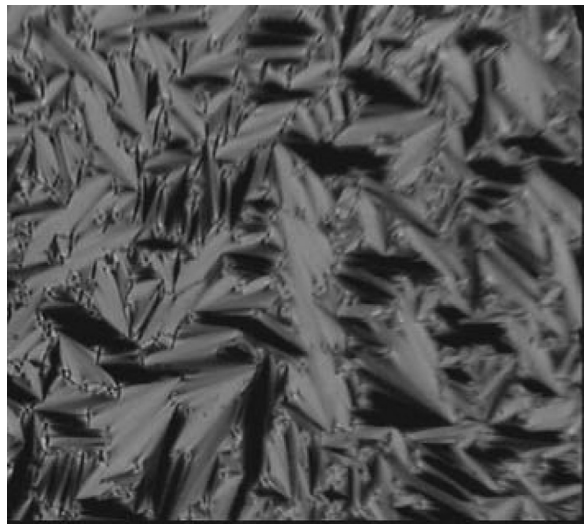

FIGURE 1 Optical photomicrograph of compound **11** exhibiting focal-conic texture (SmA) at 129.2°C.

TABLE 2 Crystal Structure Summary for Compound **5**

Empirical Formula	$C_{26}O_4H_{32}$
Formula Weight	408.54
Crystal Color, Habit	Colorless, prism
Crystal Dimensions	$0.17 \times 0.15 \times 0.10$ mm
Crystal System	Triclinic
Lattice Type	Primitive
Detector Position	45.32 mm
Pixel Size	0.137 mm
Lattice Parameters	a = 6.100(5) Å b = 11.704(10) Å c = 17.082(17) Å $\alpha = 80.85(4)^\circ$ $\beta = 85.56(4)^\circ$ $\gamma = 72.48(3)^\circ$ V = 1147.6(18) Å^3
Space Group	P-1 (#2)
Z value	2
D_{calc}	1.182 g/cm^3
F_{000}	440.00
μ(MoKα)	0.781 cm^{-1}
Detector	Rigaku Saturn
Goniometer	Rigaku AFC10
Radiation	MoKα ($\lambda = 0.71070$ Å) Graphite monochromated
Detector Aperture	70 mm × 70 mm
Data Images	720 exposures
$2\theta_{max}$	54.8°
No. of Reflections Measured	Total: 6347 Unique: 3982 ($R_{int} = 0.036$)
Corrections	Lorentz-polarization absorption (trans. factors: 0.739–0.992)
Structure Solution	Direct Methods
Refinement	Full-matrix least-squares on F^2
Function Minimized	$\Sigma\, w(F_o^2 - F_c^2)^2$
Least Squares Weights	$1/[0.0066Fo^2 + 0.9600\sigma(F_o{}^2)]/(4F_o{}^2)$
$2\theta_{max}$ Cutoff	54.8°
Anomalous Dispersion	All nonhydrogen atoms
No. Observations ($I > 2.00\sigma(I)$)	1916
No. Variables	303
Reflection/Parameter Ratio	6.32
Residuals: R1 ($I > 2.00\sigma(I)$)	0.0823
Residuals: wR_2 ($I > 2.00\sigma(I)$)	0.2121
Goodness of Fit Indicator	1.000
Max Shift/Error in Final Cycle	0.000
Maximum Peak in Final Diff. Map	0.51 e$^-$/Å^3
Minimum Peak in Final Diff. Map	−0.31 e$^-$/Å^3

term of a reduced compatibility in geometry of the branched methyl group in the terminal chain at C-4′ which is unfavorable for the non-tilting lamellar packing of molecules that give rise to the formation of smectic A phase. The textures observed under the POM at the initial heating and cooling processes can be substantiated through comparison with those analogous compounds reported in the literature [19]. The smectic A phase observed for compounds **5–11** can be clearly assigned by the formation of batonnets that coalesce to form a focal conic fan-shape texture characteristic of smectic A phase as depicted by a representative compound **11** (Fig. 1).

TABLE 3 Atomic Coordinates and $B_{iso}/B_{eq.}$ The General Temperature Factor Expression: $\exp[-2\pi^2 (a^{*2}U_{11}h^2 + b^{*2}U_{22}k^2 + c^{*2}U_{33}l^2 + 2a^*b^*U_{12}hk + 2a^*c^*U_{13}hl + 2b^*c^*U_{23}kl)]$

Atom	x	y	z	B_{eq}
O1	0.6237(6)	0.1899(3)	0.5806(2)	2.22(8)
O2	0.0514(6)	0.2640(3)	0.4465(2)	2.49(9)
O3	0.2763(6)	0.7362(3)	0.2451(2)	2.79(9)
O4	0.5135(6)	−0.1875(3)	0.7040(2)	2.64(9)
C1	0.5613(9)	0.2903(4)	0.5246(3)	2.08(12)
C2	0.3761(8)	0.3206(4)	0.4777(3)	1.76(11)
C3	0.2266(9)	0.2425(5)	0.4873(3)	2.08(12)
C4	0.2943(8)	0.1339(4)	0.5470(3)	1.76(11)
C5	0.1717(9)	0.0480(4)	0.5612(3)	2.06(12)
C6	0.2455(9)	−0.0570(5)	0.6131(3)	2.35(13)
C7	0.4512(9)	−0.0792(5)	0.6538(3)	2.03(12)
C8	0.5736(9)	0.0046(4)	0.6430(3)	2.04(12)
C9	0.4942(9)	0.1092(4)	0.5896(3)	2.03(12)
C10	0.3391(8)	0.4308(4)	0.4167(3)	2.00(12)
C11	0.5299(9)	0.4562(5)	0.3727(3)	2.30(12)
C12	0.5040(9)	0.5584(4)	0.3173(3)	2.05(12)
C13	0.2832(9)	0.6391(4)	0.3019(3)	2.05(11)
C14	0.0907(9)	0.6155(4)	0.3439(3)	2.11(12)
C15	0.1206(9)	0.5110(4)	0.4008(3)	2.02(12)
C16	0.7369(9)	−0.2247(4)	0.7380(3)	2.53(13)
C17	0.7690(10)	−0.3485(5)	0.7870(3)	2.58(13)
C18	1.0120(10)	−0.3957(5)	0.8221(3)	3.31(15)
C19	1.0620(10)	−0.5216(5)	0.8706(3)	3.25(14)
C20	1.2992(12)	−0.5630(5)	0.9067(3)	3.98(17)
C21	1.3517(15)	−0.6879(7)	0.9549(5)	6.7(2)
C22	0.0559(9)	0.8284(5)	0.2307(3)	2.64(13)
C23	0.0955(10)	0.9220(5)	0.1636(3)	2.86(14)
C24	−0.1031(10)	1.0379(5)	0.1504(3)	2.82(13)
C25	−0.0406(11)	1.1240(5)	0.0811(3)	3.36(15)
C26	−0.3217(11)	1.0116(6)	0.1321(4)	3.92(17)

TABLE 4 Selected Bond Lengths (Å), angles (°), and Torsion Angles (°) for compound **5**

O(1)-C(1)	1.369(6)	O(1)-C(9)	1.387(7)
O(2)-C(3)	1.260(7)	O(3)-C(13)	1.364(6)
O(3)-C(22)	1.458(6)	O(4)-C(7)	1.379(6)
O(4)-C(16)	1.438(7)	C(1)-C(2)	1.361(7)
C(2)-C(3)	1.458(8)	C(2)-C(10)	1.494(6)
C(3)-C(4)	1.470(6)	C(4)-C(5)	1.406(8)
C(4)-C(9)	1.399(7)	C(5)-C(6)	1.372(7)
C(6)-C(7)	1.416(8)	C(7)-C(8)	1.384(9)
C(8)-C(9)	1.386(6)	C(10)-C(11)	1.418(8)
C(10)-C(15)	1.397(6)	C(11)-C(12)	1.379(7)
C(12)-C(13)	1.409(6)	C(13)-C(14)	1.404(8)
C(14)-C(15)	1.411(7)	C(16)-C(17)	1.519(7)
C(20)-C(21)	1.515(10)	C(23)-C(24)	1.522(7)
C(24)-C(25)	1.530(8)	C(24)-C(26)	1.520(10)
C(1)-O(1)-C(9)	118.4(4)	C(13)-O(3)-C(22)	118.2(4)
C(7)-O(4)-C(16)	117.9(4)	O(1)-C(1)-C(2)	125.3(5)
C(1)-C(2)-C(3)	118.8(4)	C(1)-C(2)-C(10)	118.4(5)
C(3)-C(2)-C(10)	122.8(4)	O(2)-C(3)-C(2)	122.9(4)
O(2)-C(3)-C(4)	121.1(5)	C(2)-C(3)-C(4)	116.0(4)
C(3)-C(4)-C(5)	122.6(5)	C(3)-C(4)-C(9)	120.3(5)
C(5)-C(4)-C(9)	117.1(4)	C(4)-C(5)-C(6)	122.0(5)
C(5)-C(6)-C(7)	118.9(5)	O(4)-C(7)-C(6)	114.9(5)
O(4)-C(7)-C(8)	124.3(4)	C(6)-C(7)-C(8)	120.8(4)
C(7)-C(8)-C(9)	118.5(5)	O(1)-C(9)-C(4)	121.1(4)
O(1)-C(9)-C(8)	116.3(5)	C(4)-C(9)-C(8)	122.6(5)
C(2)-C(10)-C(11)	119.7(4)	C(2)-C(10)-C(15)	122.3(4)
C(11)-C(10)-C(15)	118.0(4)	C(10)-C(11)-C(12)	121.6(4)
C(11)-C(12)-C(13)	120.0(5)	O(3)-C(13)-C(12)	115.3(4)
O(3)-C(13)-C(14)	125.1(4)	C(12)-C(13)-C(14)	119.6(4)
C(13)-C(14)-C(15)	119.6(4)	C(10)-C(15)-C(14)	121.1(5)
O(4)-C(16)-C(17)	107.8(5)	C(16)-C(17)-C(18)	110.1(5)
C(17)-C(18)-C(19)	113.7(5)	C(18)-C(19)-C(20)	112.1(5)
C(19)-C(20)-C(21)	112.8(6)	O(3)-C(22)-C(23)	107.1(4)
C(22)-C(23)-C(24)	114.9(4)	C(23)-C(24)-C(25)	109.4(4)
C(23)-C(24)-C(26)	111.1(5)	C(25)-C(24)-C(26)	109.3(5)
C(1)-O(1)C(9)-C(8)	175.5(4)	C(9)-O(1)-C(1)-C(2)	2.2(7)
C(22)-O(3)-C(13)-C(14)	5.2(8)	C(16)-O(4)-C(7)-C(6)	170.7(4)
C(1)-C(2)-C(3)-O(2)	179.8(4)	C(1)-C(2)-C(10)-C(11)	40.3(7)
C(3)-C(2)-C(10)-C(15)	41.9(8)	C(10)-C(2)-C(3)-C(4)	176.7(4)
O(2)-C(3)-C(4)-C(9)	177.5(4)	C(3)-C(4)-C(5)-C(6)	175.4(5)
C(3)-C(4)-C(9)-O(1)	4.5(7)	O(4)-C(7)-C(8)-C(9)	178.9(4)
C(2)-C(10)-C(15)-C(14)	178.9(5)	O(3)-C(13)-C(14)-C(15)	179.4(5)
O(4)-C(16)-C(17)-C(18)	177.5(4)		

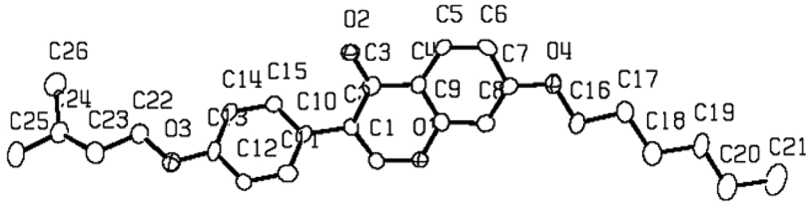

FIGURE 2 Crystal structure with atomic numbering scheme for compound **5**.

Crystal Structure Determination on Compound 5

Crystal data of compound **5** are summarized in Table 2. Whilst the atomic coordinates and B_{iso}/B_{eq} are shown in Table 3, the selected bond lengths, angles, and torsion angles are given in Table 4. The molecular structure with the atom-numbering scheme and packing of compound **5** are shown in Figures 2 and 3, respectively. It can be observed from Fig. 2 that the two phenyl rings (C1-C2-C3-C4-C9-O and C4-C5-C6-C7-C8-C9-O) are almost coplanar with a dihedral angle of 3.67°. The ring C11-C12-C13-C14-C15-C16 is twisted from the mean plane of fused-ring C1-C2-C3-C4-C9-O by 41.9(8)°. It can also be inferred from Table 4 that the endocyclic O1 atom is out-of-plane with a deviation of 2.2(7)° from the mean plane. In addition, the elongated alkyloxy chain (from C16 to C21) attached to another fused-ring C4-C5-C6-C7-C8-C9 via ether linkage is colinear with zig-zagconformation made up of methylene moiety. In general, the bond lengths and angles associated with the central core are in good agreement with those values observed in licoricone monobromoacetate [20]. However, the torsion angle (C3-C2-C10-C15) and bond length (C(2)-C(10)) as found in the present compound are less than those observed in licoricone monobromoacetate [20]. This observation can be attributed to the

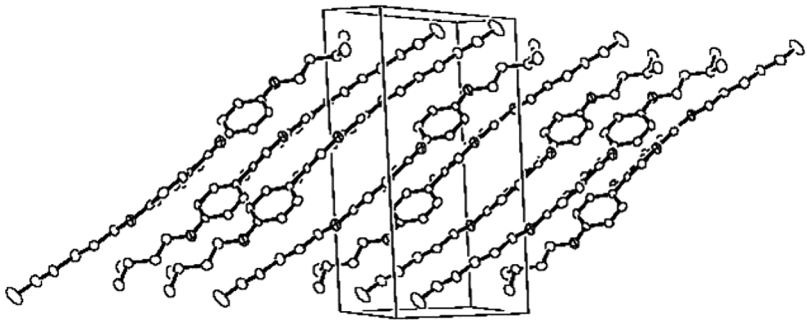

FIGURE 3 Molecular packing of compound **5** along *b* axis.

steric hindrance due to the bulky bromoacetate group at the position similar to C(15) in the present compound **5**. The crystal structure (Fig. 3) shows that the molecules lie antiparallel to each other with the molecules arranged in layers and stacked along *b* axis. The probable reason contributing to the layered structure in crystal **5** is the cohesive force resulting from dipolar or van der Waals interaction between the molecules which resemble that appeared in monomeric and dimeric imines [15, 16].

Supplementary Material

Crystallographic data for the crystal structure **5** reported in the present report have been deposited at Cambridge Crystallographic Data Centre, 12 Union Road, Cambridge CB2 1EZ, UK (CCDC 649408). The data including the structure factors are available from the corresponding author.

ACKNOWLEDGMENT

The main author (G-Y. Yeap) would like to thank Universiti Sains Malaysia and the Malaysian Government especially the Ministry of Science, Technology, and Innovation (MOSTI) for the eScience grant no. 305/PKIMIA/613315 and USM Short-Term grant no. 304/PKIMIA/638006. The authors are also grateful to the staff from the Universiti Sains Malaysia for giving indirect support to make this project a success.

REFERENCES

[1] Chudgar, N. K., Paresh, M. K., Madhavrao, S. S., & Sharma, H. C. (1995). *Liq. Cryst.*, *19*, 807.
[2] Hirose, T., Tsuya, K., Nihigaki, T., Idaka, E., & Yano, S. (1989). *Liq. Cryst.*, *4*, 653.
[3] Aldercreutz, H., Fotsis, T., Bannwart, C., Makela, T., Wahala, K., Hase, T. A., & Brunow, G. (1986). *J. Steroid Biochem.*, *25*, 791.
[4] Belmar, J., Parra, M., Zuniga, C., Perez, C., & Munoz, C. (1999). *Liq. Cryst.*, *26*, 75.
[5] Yeap, G. Y., Yam, W. S., Ito, M. M., Takahashi, Y., Nakamura, Y., Mahmood, W. A. K., Boey, P. L., Hamid, S. A., & Gorekca, E. (2007). *Liq. Cryst.*, *34*, 649.
[6] CrystalStructure 3.7.0: Crystal Structure Analysis Package, Rigaku and Rigaku/MSC (2000–2005). The Woodlands TX, USA.
[7] CRYSTALS Issue 10: Watkin, D. J., Prout, C. K., Carruthers, J. R., & Betteridge, P. W. Chemical Crystallography Laboratory, Oxford, UK. (1996).
[8] SIR2002: Burla, M. C., Camalli, M., Carrozzini, B., Cascarano, G. L., Giacovazzo, C., Polidori, G., & Spagna., R. (2003).

[9] DIRDIF99: Beurskens, P. T., Admiraal, G., Beurskens, G., Bosman, W. P., de Gelder, R., Israel, R., & Smits, J. M. M. (1999). The DIRDIF-99 program system, Technical Report of the Crystallography Laboratory, University of Nijmegen, The Netherlands.
[10] Cromer, D. T. & Waber, J. T. (1974). "International Tables for X-ray Crystallography", IV, The Kynoch Press, Birmingham, England, Table 2.2 A.
[11] Ibers, J. A. & Hamilton, W. C. (1964). *Acta Cryst.*, *17*, 781.
[12] Creagh, D. C. & McAuley, W. J. (1992). *International Tables for Crystallography*, C, Wilson, A. J. C. (Ed.), Kluwer Academic Publishers: Boston, Table 4.2.6.8, Vol. C, 219–222.
[13] Creagh, D. C. & Hubbell, J. H. (1992). *International Tables for Crystallography*, Wilson, A. J. C. (Ed.), Kluwer Academic Publishers: Boston, Table 4.2.4.3, Vol. C, 200.
[14] Choi, E. J., Ahn, J. C., Chien, L. C., Lee, C. K., Zin, W. C., Kim, D. C., & Shin, S. T. (2004). *Macromolecules*, *37*, 71.
[15] Yeap, G. Y., Ooi, W. S., Nakamura, Y., & Zhang, C. (2002), *Mol. Cryst. Liq. Cryst.*, *381*, 169.
[16] Yeap, G. Y., Hng T. C., Mahmood W. A. K., & Adnan, R. (2006). *Mol. Cryst. Liq. Cryst.*, *452*, 49.
[17] Berdagué, P., Bayle, J. P., Ho, M. S., & Fung, B. M. (1993). *Liq. Cryst.*, *14*, 667.
[18] Yeap, G. Y., Ha, S. T., Boey, P. L., Mahmood, W. A. K., Ito, M. M., & Youhei, Y. (2006). *Mol. Cryst. Liq. Cryst.*, *452*, 73.
[19] Gray, G. W. & Goodby, J. W. G. (1984). The smectic A phase. In *Smectic Liquid Crystals: Textures and Structures*, UK: Leonard Hill, 1–22.
[20] Kaneda, M., Iitaka, Y., & Shibata S. (1973). *Acta Cryst.*, *B29*, 2828.